Description of the ASEC data, its formats and locations

Table of Contents

Description of the ASEC data, its formats and locations

The Aragats Space-Environmental Center (ASEC) provides monitoring of different species of secondary cosmic rays at three altitudes. The ASEC, (Chilingarian, et al., 2003; Chilingarian, et al., 2005) consists of two high altitude stations on Mt. Aragats in Armenia and Yerevan headquarters of Cosmic Ray Division (CRD) of Yerevan Physics Institute (YerPhI). Geographic coordinates for Aragats station is 40°28'N, 44°10'E and for Nor-Amberd station is 40°22'N, 44°15'E, Yerevan - 40°11'N, 44°31'E, cutoff rigidity: ~7.1 GV, altitudes 3250m, 2000m and 1000 m correspondingly. At these 3 destinations different types of particle detectors are continuously measure the intensity of the secondary cosmic ray fluxes and send data to the Internet in real time. In this report we present short description of the ASEC detectors and data acquisition possibilities as well as obtained data structures and Internet links.

1. Aragats Solar Neutron Telescope (ASNT)

Aragats Solar Neutron Telescope (ASNT) located on the slope of the mountain Aragats in Armenia, 3250m above sea level. Geographical coordinates is 40°28'N, 44°10'E. ASNT is formed from 4 separate identical modules, as shown in Figure 1. Each module consists of standard slabs of 50x50x5 cm^3 plastic scintillators stacked vertically on a 100x100x10 cm^3 horizontal plastic scintillator slab. Scintillator slabs are fine polished to provide good optical contact of the assembly. The slab assembly (scintillator housing) is covered by white paper from the sides and bottom and firmly kept together with special belts. Total thickness of the assembly is 60 cm. Four detectors of 100x100x5 cm^3 size each located above the thick scintillator assembly as is seen in Figure 1, are used to indicate if charged particle traverse near vertically. This information is used for selecting neutral particles and “vetoing” charged particles. A scintillator light capture cones and Photo Multiplier Tubes (large cathode, FEU 49 type) are located on the top of scintillator housing in special iron shielding, where as well the Amplitude-to-digital convertor and other electronics is located.

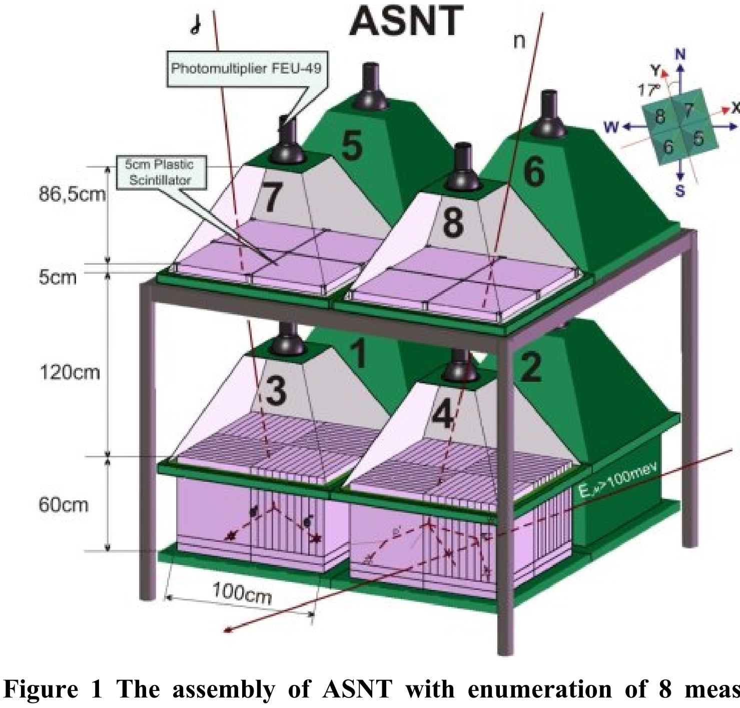

Figure 1 The assembly of ASNT with enumeration of 8 measuring channels (scintillators) and chart indicating orientation of detector axes relative to direction to the North Pole.

1.1. Structure of the information content from ASNT

Initial goal of the ASNT was to be a part of the worldwide network aimed to detect neutrons born in photosphere and reach Earth bringing direct information from its origin. The network is coordinated by the Solar-Terrestrial laboratory of the Nagoya University (Tsuchiya et al., 2001) and consists of seven same type detectors distributed at different longitudes to observe the sun 24 hours daily. In addition to the primary goal of detecting the direct neutron flux from the Sun, the SNT also has the possibility to detect charged fluxes (mostly muons and electrons) and roughly measure the direction of the incident muons. Also ASNT constitutes a central part of the new surface array to be in operation at Aragats in 2009 (see MAKET section below). The main ASNT trigger reads and stores the analog signals (PMT outputs) from all 8 channels if at least one channel reports signal. The frequency of triggers is ~4 KHz due to hit of charged and neutral particles. Big advantage of ASNT is additional, so called, software triggers, exploiting the information from Amplitude-Digital-Converters (ADC) on energy releases in scintillators.

This, additional information, not assessable yet from other particle detectors from world-wide networks, allows as we will see, solving additional physical problems. The software triggers are not fixed in electronics and it is possible to remote add or change them very flexible. The list of available information from modernized ASNT is as follows:

1. 1 minute count rates (easily can be changed to 10 seconds, or to another time span) of all 8 channels of ASNT (see Table 1, Figure 2);
2. Count rates from
3. different incident directions separately, 16 possible coincidences of 4 upper and 4 bottom scintillators are related to 9 different directions (see Table 2);
4. Count rates of the special coincidences (see details in Table 3, Figure 3);
5. Estimates of the variances of count rates of each ASNT channel, variances are calculated by 12 five-second count rates (see Table 4, Figure 4);
6. 8 x 8 correlation matrix of ASNT channels calculated by five-second count rates in 1 minute (see Table 5);
7. Count rates correspondent to old SNT 4 threshold on the energy release in thick scintillators (see Table 6);
8. The same as in previous point put only for particles that did not registered in upper layer (veto on charged particles to select samples enriched by neutrons) (see Table 6);
9. Histograms of energy releases in all 8 channels of ASNT (see Figure 5);
10. The same as in previous point with invoking veto option;
11. Time and values of energy releases in ASNT channels conditioned on existence of signals in all 8 scintillators, so called, EAS trigger (accuracy of time stamp is ~50 μsec), (Figure 6);
12. Energy releases in upper or bottom scintillators conditioned on absence of signal in correspondingly down and upper layers and on minimal energy release, i.e. horizontal muon trigger.

We use XML format of data, allowing metafiles with detailed information about detector location, and operation conditions. After transfer by wireless connections to CRD headquarters in Yerevan the data are archived and stored in MySQL data base. The main data analysis platform, Data Visualization Interactive Network (DVIN (Eghikyan and Chilingarian, 2005)) now is operated with data in XML format and allow us download data also in ASCII format.
All raw data in the XML format is available from HTTP server at CRD headquarters in Yerevan from the link.

http://crdlx5.yerphi.am/ASEC_Data/ADAS/asnt/snt

In the directory “DEFOULT” following information is stored:

1. snt (columns 1-8) - the count rates of all 8 ASNT channels: first 4 columns – from 60 cm scintillators, 5-8 columns – from 5 cm scintillator. The numbering of scintillators is explained in the Figure 1. The count rates are posted in the Table 1;
2. snt (columns 9-24) – the count rates corresponding to the 16 coincidences in upper and bottom ASNT layers, i.e. – corresponding to the traversal of the single charged particle (the probability that neutron will generate energy release in 5 cm scintillator is rather small). The order of the different directions in the file is following: [1-5] [1-6] [1-7] [1-8] [2-5] [2-6] [2-7] [2-8] [3-5] [3-6] [3-7] [3-8] [4-5] [4-6] [4-7] [4-8], where the first number corresponds to the lower layer and the second – to the upper (see Figure 1) Also on the same Figure you can see the orientation of ASNT axes according to direction to the North Pole, thus we can calculate the interval of the horizontal angles of incidence related to each coincidence.
3. snt (columns 25-31) – the count rates of the "special" coincidences different from listed above and forming the "full system" of possible configurations of the channel operation. Conditioned on the existing as minimum 1 signal in 8 ASNT channels there could be the following possibilities of number of counts in top and bottom layers (the first sign in the pair is corresponding to the bottom thick scintillator): many-many [m-m] (more than one count in 4 bottom and 4 top layers), many-zero [m-z] (more than 1 in bottom and nothing in 4 top), zero-many [z-m], zero-one [z-o], one-zero [o-z], many-one [m-o], one-many [o-m]. The fraction of the "special" coincidences relative to the "main" trigger is posted in the Table 3 the time-series of the s "special" triggers are posted in the Figure 3.
4. snt (columns 32) - the number of the "main" triggers – at least one signal in 8 channels in preselected time span (1 minute). If we consider all logical configurations of ASNT operation outcomes, this number will be equal to sum of the columns 9-31. As we mention already the number of triggers is ~ 4 KHz, dependent on the hardware settings: PMT high voltage and threshold of channel "firing".
5. snt (columns 33-40) - the variances of 8 channels, see Table 4 and Figure 4;
6. snt (columns 41-68) – the correlation matrix, see Table 5.

In the directories "spectrum" following information is stored:

1. spectrum1, … spectrum4 the histograms of the energy releases in thick 60 cm scintillator;

In files with extension;

2. spectrum5, … spectrum8 the histograms of energy releases in 5 cm thin scintillators;
3. spectrum9,..., spectrum12 histograms of energy releases in 60 cm thick scintillators (with invoking veto option on the charged particles in the upper "anticoincidence" shielding);

By integrating the histograms spectrum1,..., spectrum4 and spectrum9,...,spectrum12 we calculate the count rates according to 4 predefined thresholds on the value of the energy release (PMT output), to continue time series in the same data format as old version of ASNT started from 1996 (http://crd.aragats.am/DVIN/). As a first (or zero- threshold) we use the sum of all channels of the histogram. To get number of particles with Threshold 1 we must calculate sum of the channels of the histogram from 16 to 127. For the Threshold 2 – sum of the 23-127 channels, Threshold 3 – 27-127 channels and Threshold 4 – 31-127 channels.

To calculate count rate of the particles with thresholds for the detector 1-4 (60cm) we need spectrums 1-4 files. To calculate count rate of the particles with veto for the detector 1-4 we need spectrums 9-12 files (see Table 6).

The CRD "ARSRV" local file server contain files with following information:

1. The detailed information on the many-many case: the time stamp and energy releases in all 8 ASNT cannels. This case is related to the Extensive Air Showers (EAS), when energy of primary particle is high enough to generate particle cascade with numerous secondary particles reaching earth surface. By selecting different subsamples of many-many case according to the number of detected secondary particles (energy releases) we can select

events with different primary energy, thus constructing the energy spectra of the primary particles. The calibration of the ASNT can be done with MAKET-ANI EAS array (Chilingarian, et al., 2004). In the Figure 6 the time series of the count rates correspondent to different energy releases are posted.

2. Another kind of events stored in the files with "events" extension is related to the horizontal muon traversal. The logical software trigger selects events when there are more than 2 signals in top or bottom layers only, i.e. selecting horizontally traversing particle, or group of particles. The additional condition of large energy release (the code >25) is rejecting coincidences of the vertical traversal of low energy particles. The acceptance of the system of bottom thick scintillators is rather large ~(+/- 8.5^0), the acceptance of very narrow system of the top thin scintillators will select horizontal muons within ~(+/- 0.7^0) of zenith angles.

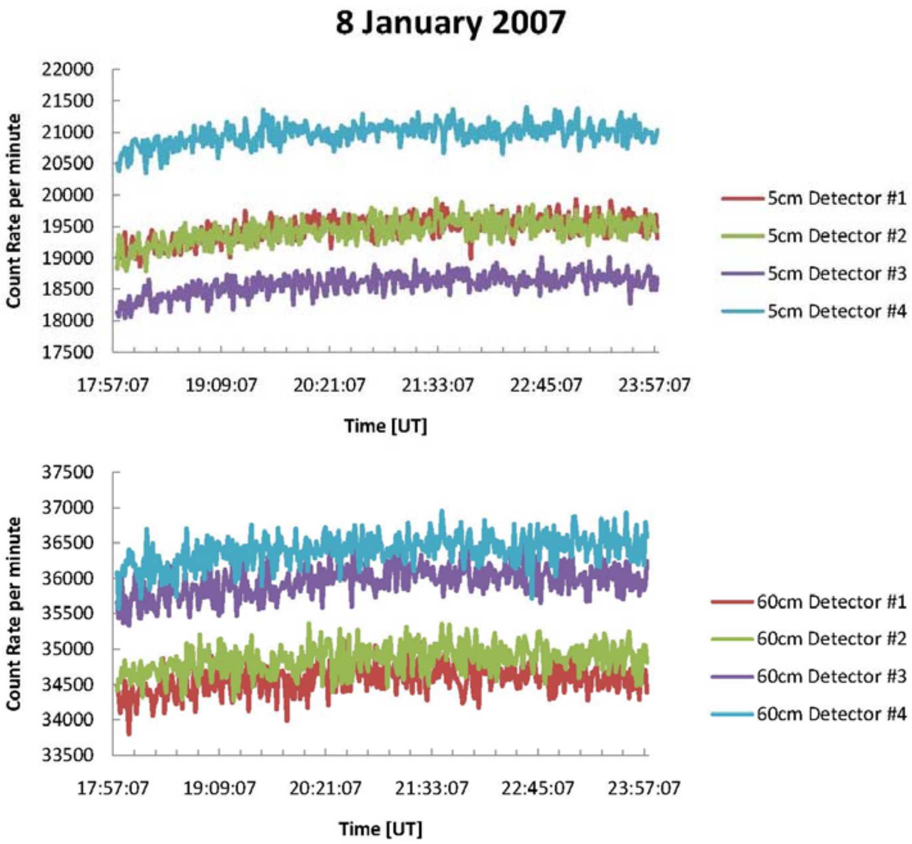

Figure 2: Time series of count rates of 8 ASNT channels. The difference of mean values is due to peculiarities of PMT used.

Table 1: Count rates of the ASNT channels, variances and relative errors (07.02.2008).

Detector	Average	Standard deviation	Relative error [%]
60cm Detector 1	34465	244	0.70
60cm Detector 2	33027	238	0.72
60cm Detector 3	34864	238	0.68
60cm Detector 4	35235	252	0.71
SUM 60 cm	**141784**		
5cm Detector 5	22254	178	0.80
5cm Detector 6	19775	201	1.01
5cm Detector 7	22315	178	0.80
5cm Detector 8	20871	209	1.00
SUM 5 cm	**78459**		

Table 2: Mean count rates related to the different incident directions, variances, relative errors and fractions according the number of "main" triggers (181474/ minute). φ is true north-based azimuth angle, θ is zenith angle (07.02.2008).

Direction		Average	Standard deviation	Relative error [%]	Fraction
Vertical Directions	[1-5]	3965	70	1.77	1.66
	[2-6]	2899	76	2.66	1.67
	[3-7]	3754	68	1.83	1.39
	[4-8]	3128	79	2.54	1.86
$\varphi=73^0\pm31^0$ E $\theta=30^0\pm11^0$	[1-6]	1278	37	2.92	0.69
	[3-8]	1306	38	2.98	0.73
$\varphi=163^0\pm31^0$ E $\theta=30^0\pm11^0$	[1-7]	1544	40	2.64	0.67
	[2-8]	1346	40	3.01	0.80
$\varphi=253^0\pm31^0$ E $\theta=30^0\pm11^0$	[2-5]	1458	38	2.64	0.74
	[4-7]	1496	39	2.63	0.67
$\varphi=343^0\pm31^0$ E $\theta=30^0\pm11^0$	[3-5]	1454	38	2.67	0.68
	[4-6]	1267	38	3.00	0.72
$\varphi=118^0\pm20^0$ E $\theta=38^0\pm10^0$	[1-8]	691	27	4.00	0.39
$\varphi=208^0\pm20^0$ E $\theta=38^0\pm10^0$	[2-7]	672	26	3.86	0.33
$\varphi=28^0\pm20^0$ E $\theta=38^0\pm10^0$	[3-6]	591	25	4.27	0.33
$\varphi=298^0\pm20^0$ E $\theta=38^0\pm10^0$	[4-5]	730	27	3.83	0.37
SUM		**27579**			**13.70**

Table 3: Mean count rates of "special" cases; variances, relative errors and fractions according the number of "main" triggers (181474/ minute) (07.02.2008).

Coincidence	Average	Standard deviation	Relative error [%]	Fraction
Many – Many	568	24	4.27	0.31
Many – Zero	5536	87	1.58	3.33
Zero – Many	759	28	3.78	0.33
Zero – One	51735	274	0.53	26.57
One – Zero	93191	345	0.37	54.55
Many – One	1551	47	3.05	0.90
One – Many	690	29	4.20	0.32
SUM	**154030**			**86.30**

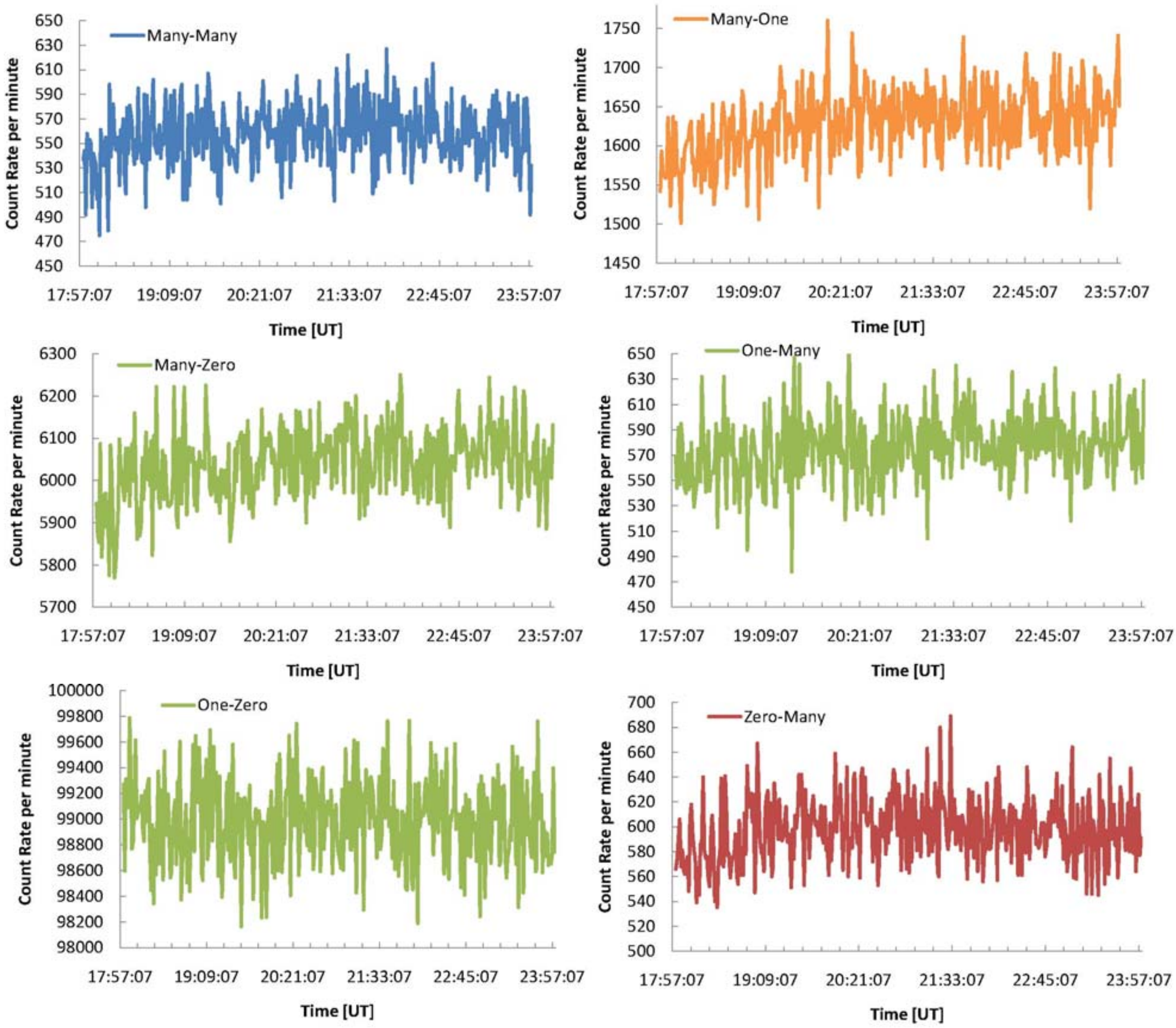

Figure 3: Time series of the "special" cases, see description in the in the text and in the Table 2.

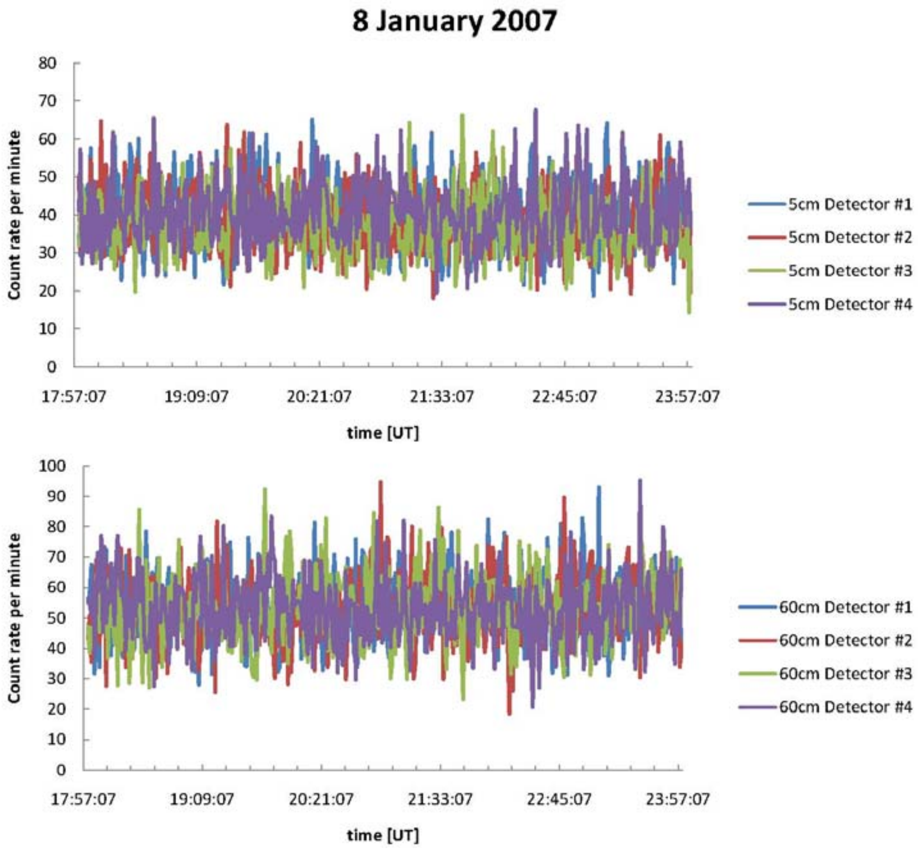

Figure 4: Time series of the ASNT channel variances. Despite the mean values of ASNT channels slightly differ, the variances are very close to each-other, thus proving uniformity of ASNT channels.

Table 4: Mean value of the variance, its variance and relative error calculated by 5-sec count rates of 1 minute time span (total 12 5-dec count rates) (07.02.2008).

Detectors	Average	Standard deviation	Relative error [%]
60cm Detector 1	52	11	21.36
60cm Detector 2	50	10	21.36
60cm Detector 3	51	11	21.71
60cm Detector 4	52	11	21.71
5cm Detector 1	42	9	21.30
5cm Detector 2	39	8	21.00
5cm Detector 3	42	9	21.36
5cm Detector 4	40	9	21.69

Table 5: Mean value of the correlation matrix, calculated by 5-sec count rates of 1 minute time span and averaged over time span of 6 hours at 7 January 2008. Emphasized (red) values are related to ASNT channels stacked one above another, for which correlation should be non zero.

	Det 1	Det 2	Det 3	Det 4	Det 5	Det 6	Det 7	Det 8
Det 1	1							
Det 2	0.041	1						
Det 3	0.042	-0.003	1					
Det 4	-0.003	0.032	0.042	1				
Det 5	0.154	0.067	0.049	0.024	1			
Det 6	0.066	0.118	0.006	0.053	0.015	1		
Det 7	0.053	0.027	0.135	0.049	0.022	-0.007	1	
Det 8	0.048	0.052	0.057	0.122	0.021	0.018	0.023	1

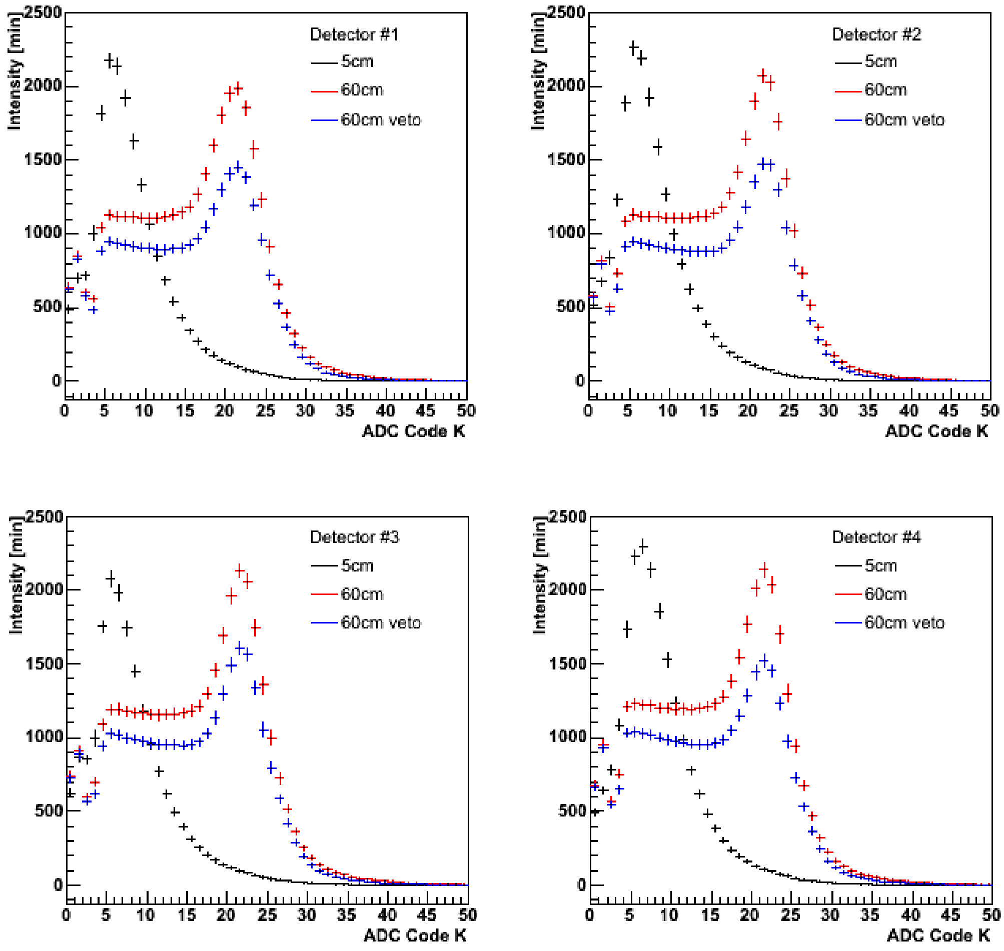

Figure 5: Spectra of the energy releases in thick and thin scintillators. Veto option suppresses contamination of the charged particles by ~25%.

Table 6: Count rates correspondent to old SNT 4 threshold on the energy release in thick scintillators.

Threshold	Average		Standard deviation		Relative error [%]	
		Veto		Veto		Veto
Threshold1	78586	58705	551.77	300.14	0.70	0.51
Threshold2	34460	25737	895.00	587.74	2.60	2.28
Threshold3	10550	7725	353.88	268.68	3.35	3.48
Threshold4	4410	2866	139.61	99.23	3.17	3.46

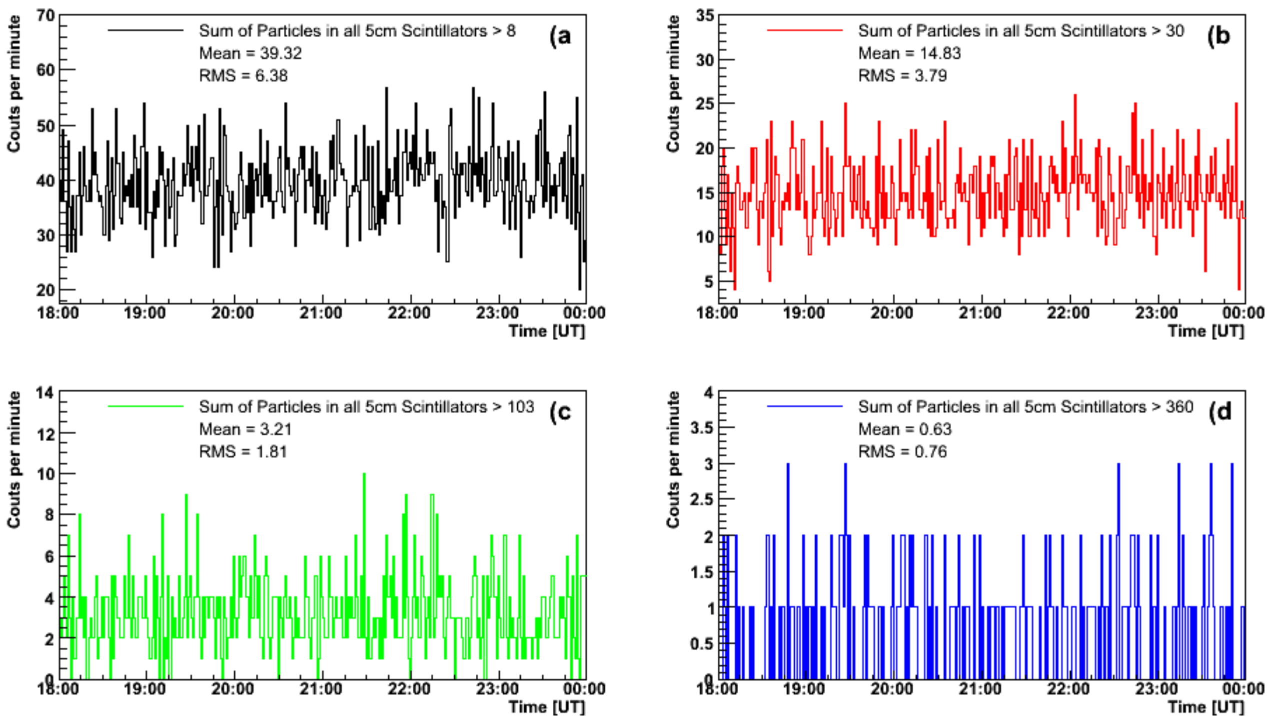

Figure 6: The time series of the EAS initiated triggers (many-many case) conditioned on the value of the minimal number of incident particles (shown in the Figures) in 5 cm scintillator.

2. Nor-Amberd Multidirectional Muon Monitor (NAMMM)

Nor-Amberd Multidirectional Muon Monitor (NAMMM) (Dorman 1975; Beglaryan, et al., 1989) located on the slope of the mountain Aragats in Armenia, at 2000m above sea level. Geographical coordinates is 40°22'N, 44°15'E. The NAMMM, shown in Figure 7 consists of two layers of plastic scintillators above and below two of the three sections of the Nor Amberd Neutron Monitor (NM). The lead (Pb) filter of the NM absorbs electrons and low energy muons. The threshold energy of the detected muons is estimated to be ~250 MeV. The NAMMM consists of 6 up and 6 down scintillators, each having the area of 0.8 m^2. The distance between layers is ~ 1 m., and the interval of zenith angles determined by the paired coincidences of upper and lower scintillators is not greater than 25º. The data acquisition system of the NAMMM, the same as ASNT, can register all coincidences of detector signals from the upper and lower layers, thus, enabling measurements of the arrival of the muons from different directions.

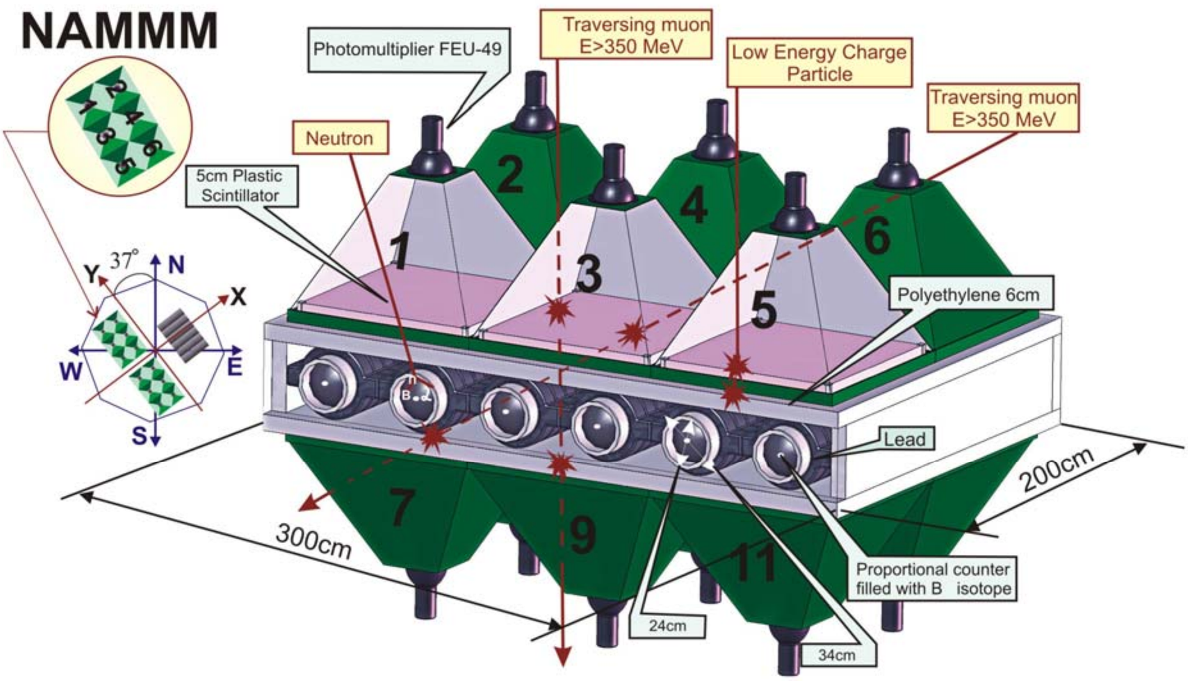

Figure 7 Nor-Amberd Multidirectional Muon Monitor (NAMMM), section 1

2.1. Structure of the information content from NAMMM

The list of available information from NAMMM is as follows:

- 1 minute count rates (easily can be changed to 10 seconds, or to another time span) of all 12 channels of NAMMM (see Table 7);
- Count rates of different incident directions separately, 36 possible coincidences of 6 upper and 6 bottom scintillators are related to 15 different directions (see Table 9);
- Count rates of the special coincidences (see details in Table 11);
- 1 minute estimates of the variances of count rates of each NAMMM channel, variances are calculated by 12 five-second count rates (see Table 12);
- 12 x 12 correlation matrix of NAMMM channels calculated by five-second count rates in 1 minute (see Table 13);

The raw data of the two sections of NAMMMs in the XML format available from CRD http server.

http://crdlx5.yerphi.am/ASEC_Data/ADAS/nammm/nammm1
http://crdlx5.yerphi.am/ASEC_Data/ADAS/nammm/nammm2

In the directory "DEFAULT" of both mentioned links the following information is stored correspondingly for the first and second sections of detector, namely NAMMM1 and NAMMM2:

- columns 1-12 - the count rates of all channels of NAMMM: first 6 columns – from upper layer scintillators, 7-12 columns – from lower layer scintillator. The numbering of scintillators is explained in the Figure 7. The count rates are posted in the Table 7;
- columns 13-48 – the count rates corresponding to the 36 coincidences in upper and lower NAMMM layers, i.e. – corresponding to the traversal of the single charged particle (mostly muons with energy > 250 MeV). The order of the different directions in the file is following: [1-7] [1-8] [1-9] [1-10] [1-11] [1-12] [2-7] [2-8] [2-9] [2-10] [2-11] [2-12] [3-7] [3-8] [3-9] [3-10] [3-11] [3-12] [4-7] [4-8] [4-9] [4-10] [4-11] [4-12] [5-7] [5-8] [5-9] [5-10] [5-11] [5-12] [6-7] [6-8] [6-9] [6-10] [6-11] [6-12], where the first number corresponds to the upper layer and the second – to the lower (see Figure 7) Also on the same Figure you

can see the orientation of NAMMM axes according to direction to the North Pole, thus we can calculate the interval of the horizontal angles of incidence related to each coincidence.
- columns 49-55 – the count rates of the "special" coincidences different from listed above and forming the "full system" of possible configurations of the channel operation. Conditioned on the existing as minimum 1 signal in 12 NAMMM channels there could be the following possibilities of number of counts in top and bottom layers (the first sign in the pair is corresponding to the upper scintillator): many-many (more than one count in 6 top and 6 bottom layers), many-zero (more than 1 in top and nothing in 6 bottom), zero-many, zero-one, one-zero, many-one, one-many. The fraction of the "special" coincidences relative to the "main" trigger is posted in the Table 11.
- columns 56 - the number of the "main" triggers – at least one signal in 12 channels in preselected time span (1 minute). If we consider all logical configurations of NAMM operation outcomes, this number will be equal to sum of the columns 13-55.
- columns 57-68 - the variances of 12 channels, see Table 12;
- columns 69-134 – the correlation matrix, see Table 13.

In the directories "spectrum" the 127-channel histograms of the energy releases are stored for each minute, in files with extensions:

- spectrum1 - spectrum6, the histograms of the energy releases in the upper scintillators are stored.
- spectrum7 - spectrum12, the histograms of the energy releases in the lower scintillators are stored;
- spectrum13 - spectrum18, histograms of energy releases, in upper detectors are stored with condition that in lower detectors there was now signal, i.e., the energy releases of electrons and low energy muons filtered in the lead absorber.

The information on the spectra of energy releases is essential for the continuous calibration of the all measuring channels. As one can see in Figure 8 the maximum of smoothed histograms are in the region 10-11 MeV, and this value should be monitored and kept constant during multiyear detector operation. In Figure 8 are presented 1-minute spectra summed over all four detectors and averaged over several hours. The blue curve is energy releases of the low energy muons and electrons (spectrum13-18) and the red curve is corresponding to high energy muons (subtracting from spectrum 1-6, spectrums 13-18). We can see than high energy muons in average can give much higher energy releases comparing with low energy muons and electrons. This additional information can be useful if Ground Level Enhancements (GLE) was originated by the primary particles having higher energy comparing with the GCR flux. Additionally to enhancement of the count rate we may notice some unusual features in the histograms of energy releases.

Table 7 Count Rates of the NAMMM1 channels and variances (25-01-2008; 14:00-19:00).

Detectors	Average	Standard deviation	Relative Error (%)
Detector 1	14660	118	0.80
Detector 2	14667	120	0.82
Detector 3	15409	121	0.79
Detector 4	16665	130	0.78
Detector 5	17480	147	0.84
Detector 6	16526	125	0.76
SUM of upper layer	**89528**		
Detector 7	9327	100	1.07
Detector 8	10554	103	0.98
Detector 9	9143	92	1.01
Detector 10	8581	97	1.13
Detector 11	9250	106	1.15
Detector 12	10459	99	0.95
SUM of lower layer	**54658**		

Table 8 Count Rates of the NAMMM2 channels and variances (25-01-2008; 14:00-23:00).

Detectors	Average	Standard deviation	Relative Error (%)
Detector 1	14619	100.09	0.68
Detector 2	15526	128.45	0.83
Detector 3	15970	107.3	0.67
Detector 4	15893	103.18	0.65
Detector 5	15887	128.36	0.81
Detector 6	14627	129.3	0.88
SUM of upper layer	**92192**		
Detector 7	9277	108.56	1.17
Detector 8	8823	110.01	1.25
Detector 9	9729	94.06	0.97
Detector 10	10225	132.03	1.29
Detector 11	9090	88.63	0.98
Detector 12	9621	112.76	1.17
SUM of lower layer	**55642**		

Table 9 Mean count rates related to the different incident directions detected by the NAMMM1; variances, relative errors and fractions according the number of the “main” triggers (113109/ minute). Angle φ calculated relative XY axes (see Figure 7); φ is true north-based azimuth angle, θ is zenith angle.

Directions		Average	Standard deviation	Relative Error (%)	SUM
Vertical	[1-7]	2459	52	2.11	15509
	[2-8]	2621	53	2.02	
	[3-9]	2641	51	1.93	
	[4-10]	2313	49	2.12	
	[5-11]	2693	53	1.97	
	[6-12]	2782	49	1.76	
$\varphi=53^0\pm28^0$ E $\theta=37^0\pm13^0$	[1-8]	504	24	4.76	1538
	[3-10]	494	22	4.45	
	[5-12]	539	22	4.08	
$\varphi=233^0\pm28^0$ E $\theta=37^0\pm13^0$	[2-7]	955	29	3.04	3070
	[4-9]	1112	36	3.24	
	[6-11]	1003	32	3.19	
$\varphi=323^0\pm30^0$ E $\theta=37^0\pm13^0$	[3-7]	751	29	3.86	3092
	[4-8]	833	28	3.36	
	[5-9]	753	27	3.59	
	[6-10]	755	28	3.71	
$\varphi=143^0\pm30^0$ E $\theta=37^0\pm13^0$	[1-9]	689	27	3.92	2694
	[2-10]	583	25	4.29	
	[3-11]	724	26	3.59	
	[4-12]	699	26	3.72	
$\varphi=98^0\pm25^0$ E $\theta=49^0\pm11^0$	[1-10]	155	12	7.74	349
	[3-12]	194	14	7.22	
$\varphi=278^0\pm18^0$ E $\theta=49^0\pm10^0$	[4-7]	357	18	5.04	699
	[6-9]	341	19	5.57	
$\varphi=188^0\pm18^0$ E $\theta=49^0\pm10^0$	[2-9]	321	19	5.92	647
	[4-11]	326	18	5.52	
$\varphi=8^0\pm25^0$ E $\theta=49^0\pm11^0$	[3-8]	219	14	6.39	420
	[5-10]	201	14	6.97	
$\varphi=143^0\pm13^0$ E $\theta=61^0\pm6^0$	[1-11]	49	6	12.24	101
	[2-12]	52	7	13.46	
$\varphi=323^0\pm13^0$ E $\theta=61^0\pm6^0$	[5-7]	53	7	13.21	115
	[6-8]	61	7	11.48	
$\varphi=116^0\pm12^0$ E $\theta=64^0\pm6^0$	[1-12]	28	6	21.43	28
$\varphi=296^0\pm12^0$ E $\theta=64^0\pm6^0$	[6-7]	34	6	17.65	34
$\varphi=170^0\pm12^0$ E $\theta=64^0\pm6^0$	[2-11]	34	6	17.65	34
$\varphi=350^0\pm12^0$ E $\theta=64^0\pm6^0$	[5-8]	32	5	15.63	32
	SUM	**28360**			

Table 10 Mean count rates related to the different incident directions detected by the NAMMM2; variances, relative errors and fractions according the number of the "main" triggers (113109/ minute). Angle φ calculated relative XY axes (see Figure 7); φ is true north-based azimuth angle, θ is zenith angle.

Directions		Average	Standard deviation	Relative Error (%)	SUM
Vertical	[1-7]	2318	48.44	2.09	15406
	[2-8]	2251	47.98	2.13	
	[3-9]	2779	54.52	1.96	
	[4-10]	2679	48.96	1.83	
	[5-11]	2667	48.96	1.84	
	[6-12]	2711	53.19	1.96	
$\varphi=53^0\pm28^0$ E $\theta=37^0\pm13^0$	[1-8]	481	21.44	4.46	1525
	[3-10]	517	22.8	4.41	
	[5-12]	527	22.37	4.24	
$\varphi=233^0\pm28^0$ E $\theta=37^0\pm13^0$	[2-7]	990	32.31	3.26	3261
	[4-9]	1130	32.92	2.91	
	[6-11]	1141	33.52	2.94	
$\varphi=323^0\pm30^0$ E $\theta=37^0\pm13^0$	[3-7]	665	26.15	3.93	2766
	[4-8]	667	26.26	3.94	
	[5-9]	711	26.63	3.75	
	[6-10]	724	26.34	3.64	
$\varphi=143^0\pm30^0$ E $\theta=37^0\pm13^0$	[1-9]	815	27.29	3.35	3229
	[2-10]	777	27.48	3.54	
	[3-11]	836	28.17	3.37	
	[4-12]	800	28.01	3.50	
$\varphi=98^0\pm25^0$ E $\theta=49^0\pm11^0$	[1-10]	192	13.83	7.20	400
	[3-12]	208	13.24	6.37	
$\varphi=278^0\pm18^0$ E $\theta=49^0\pm10^0$	[4-7]	321	17.88	5.57	660
	[6-9]	339	18.97	5.60	
$\varphi=188^0\pm18^0$ E $\theta=49^0\pm10^0$	[2-9]	385	20	5.19	778
	[4-11]	393	19.76	5.03	
$\varphi=8^0\pm25^0$ E $\theta=49^0\pm11^0$	[3-8]	183	13.51	7.38	364
	[5-10]	181	13.46	7.44	
$\varphi=143^0\pm13^0$ E $\theta=61^0\pm6^0$	[1-11]	56	7.53	13.45	114
	[2-12]	58	7.79	13.43	
$\varphi=323^0\pm13^0$ E $\theta=61^0\pm6^0$	[5-7]	47	7.36	15.66	95
	[6-8]	48	6.87	14.31	
$\varphi=116^0\pm12^0$ E $\theta=64^0\pm6^0$	[1-12]	28	5.27	18.82	28
$\varphi=296^0\pm12^0$ E $\theta=64^0\pm6^0$	[6-7]	32	5.92	18.50	32
$\varphi=170^0\pm12^0$ E $\theta=64^0\pm6^0$	[2-11]	39	6.34	16.26	39
$\varphi=350^0\pm12^0$ E $\theta=64^0\pm6^0$	[5-8]	26	5.29	20.35	26
	SUM	**28722**			

Table 11 Mean count rates of “special” cases (NAMMM1) ; variances, relative errors and fractions according the number of “main” triggers (113109/ minute).

Coincidence	Average	Standard deviation	Relative Error [%]
Many – Many	39	6.11	15.67
Many – Zero	1790	43.44	2.43
Zero – Many	322	17.55	5.45
Zero – One	27469	168.89	0.61
One – Zero	62117	248.32	0.40
Many – One	376	19.26	5.12
One – Many	170	12.64	7.44

Table 12 Mean values of the count rates and variances, calculated by 5-sec count rates of 1 minute time span (total 12 5-dec count rates) (NAMMM1).

Detectors	Mean value of the count rate	Mean value of the variance	Relative error (variance/count rate)
Detector 1	1272	15.95	0.0125
Detector 2	1191	15.34	0.0129
Detector 3	1044	14.40	0.0138
Detector 4	1287	16.02	0.0124
Detector 5	1269	15.87	0.0125
Detector 6	1284	15.94	0.0124
Detector 7	811	12.69	0.0156
Detector 8	923	13.53	0.0147
Detector 9	690	11.63	0.0169
Detector 10	735	12.03	0.0164
Detector 11	749	14.81	0.0197
Detector 12	780	12.43	0.0159

Table 13 Mean value of the correlation matrix, calculated by 5-sec count rates of 1 minute time span and averaged over time span of 5 hours at 25 January 2008. Emphasized (red) values are related to NAMMM1 channels stacked one above another, for which correlation should be significant.

	Det 1	Det 2	Det 3	Det 4	Det 5	Det 6	Det 7	Det 8	Det 9	Det 10	Det 11	Det 12
Det 1	1											
Det 2	0.014	1										
Det 3	0.011	0.017	1									
Det 4	0.001	0.006	-0.010	1								
Det 5	0.018	-0.027	-0.009	0.013	1							
Det 6	0.001	0.038	0.010	0.015	0.023	1						
Det 7	**0.209**	0.072	0.080	0.015	-0.004	0.008	1					
Det 8	0.004	**0.213**	0.035	0.034	0.012	0.018	-0.000	1				
Det 9	0.056	0.044	**0.216**	0.085	0.063	0.009	-0.000	0.005	1			
Det 10	0.015	0.045	0.013	**0.166**	0.006	0.066	-0.030	-0.004	0.005	1		
Det 11	-0.005	0.010	0.067	0.040	**0.217**	0.077	-0.020	0.018	0.022	-0.001	1	
Det 12	0.000	0.006	0.051	0.051	0.029	**0.191**	0.002	0.027	0.003	0.020	0.007	1

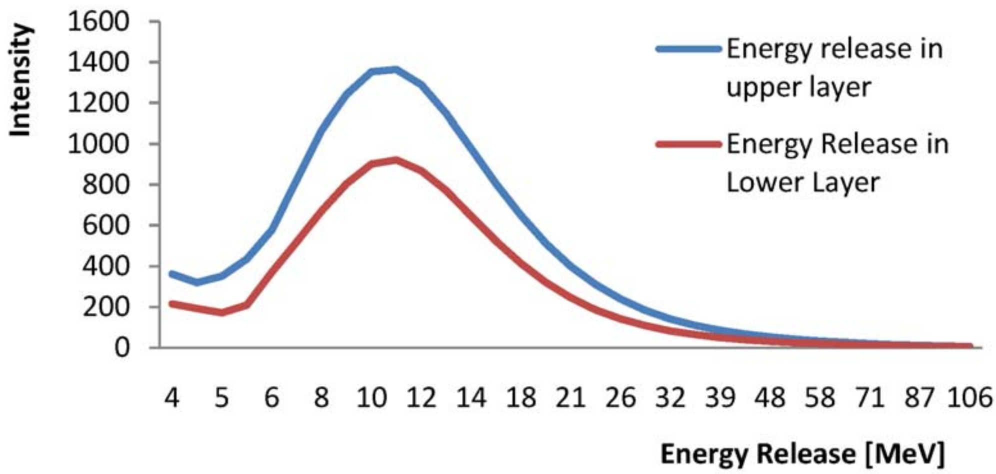

Figure 8 Histogram of energy releases in NAMMM1 upper and lower scintillators (1 minute data).

3. Nor-Amberd and Aragats Neutron Monitors (NANM & ArNM)

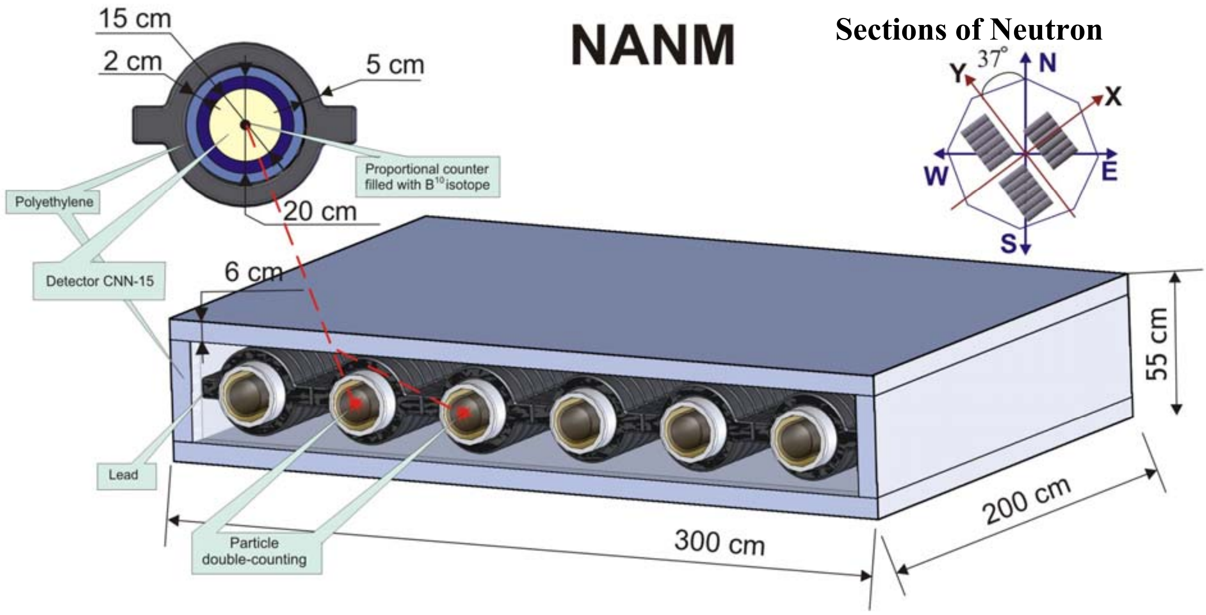

Figure 9 Nor-Amberd Neutron Monitor (NANM)

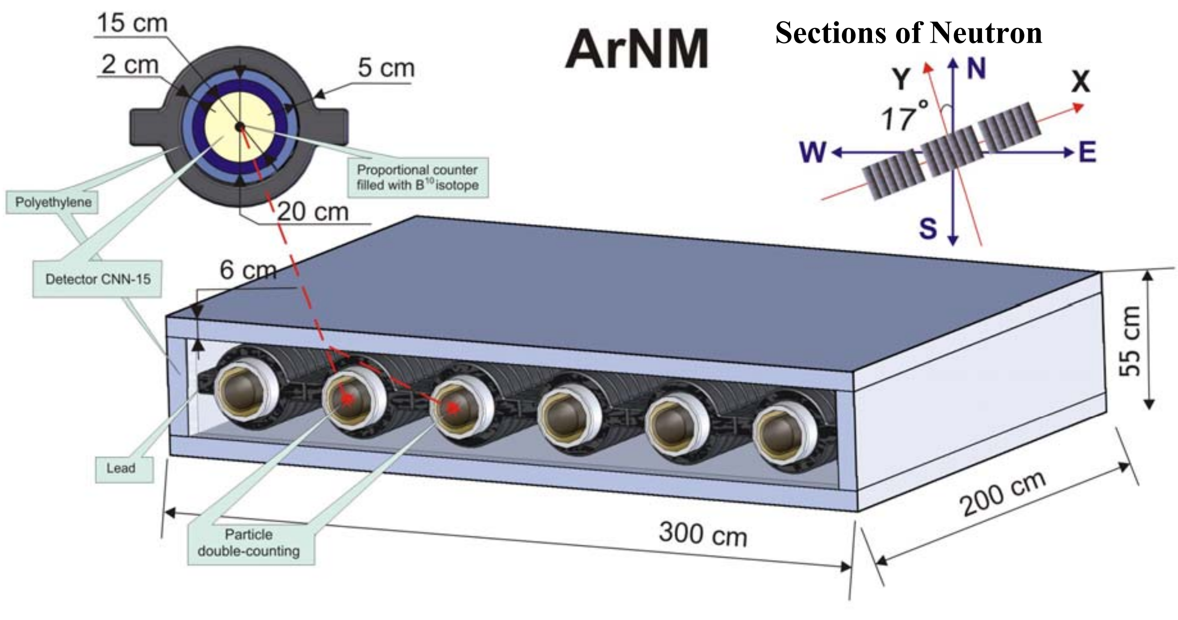

Figure 10 Aragats Neutron Monitor (ArNM).

Two 18NM-64 neutron monitors (see Figure 9, Figure 10) (Moraal, et al., 2000), are in operation at Nor-Amberd (40°22'N, 44°15'E, 2000m above sea level), and at Aragats, (40°28'N, 44°10'E, 3250m above sea level) research stations. They called the Nor Amberd Neutron Monitor (NANM), and the Aragats Neutron Monitor (ArNM), respectively. The monitors are equipped with new electronics providing time integration of counts by three dead times. The first dead time equals to 400ns for collecting almost all thermalized neutrons entering the proportional chamber from the lead. The second dead time is equal to the 0.25ms and the third one equal 1.25ms (as most of NM from world-wide network). Also 2 proportional chambers without lead coverage are added to NANM.

The raw data of the NANM and ArNM is available from CRD http server by these links:

http://crdlx5.yerphi.am/ASEC_Data/ADAS/nanm/nanm/DEFAULT/

http://crdlx5.yerphi.am/ASEC_Data/ADAS/arnm/arnm/DEFAULT/

In the data files of the NM following information is stored (Table 14 and Table 15):

1. columns 1+3i (i=0,…,17) - the count rates of all 18 channels of NM with dead time 400ns.
2. columns 2+3i (i=0,…,17) - the count rates of all 18 channels of NM with dead time 0.25ms.
3. columns 3+3i (i=0,…,17) - the count rates of all 18 channels of NM with dead time 1.25ms.
4. column 55 – the pressure coefficient.
5. columns 56 – 60 yet unused channels, additional neutron detectors to be attached soon.

Table 14. Count rates of the 18 channels of the NANM (07.02.2008).

	Number of Column	Average Count Rate (0.4us)	Std. Dev.	SUM	**Number of Column**	Average Count Rate (250us)	Std. Dev.	SUM	**Number of Column**	Average Count Rate (1250us)	Std. Dev.	SUM
Detector 1	**1**	1530	57	**27483**	**2**	1312	39	**23993**	**3**	1172	33	**21633**
Detector 2	**4**	1375	47		**5**	1216	37		**6**	1101	32	
Detector 3	**7**	1608	52		**8**	1405	40		**9**	1262	35	
Detector 4	**10**	1628	52		**11**	1425	39		**12**	1277	33	
Detector 5	**13**	1580	53		**14**	1379	41		**15**	1243	35	
Detector 6	**16**	1391	64		**17**	1198	37		**18**	1082	32	
Detector 7	**19**	1676	54		**20**	1455	41		**21**	1310	34	
Detector 8	**22**	1608	51		**23**	1412	41		**24**	1268	35	
Detector 9	**25**	1539	50		**26**	1345	38		**27**	1215	32	
Detector 10	**28**	1553	53		**29**	1361	41		**30**	1228	35	
Detector 11	**31**	1592	54		**32**	1370	41		**33**	1232	35	
Detector 12	**34**	1417	49		**35**	1236	38		**36**	1114	32	
Detector 13	**37**	1471	51		**38**	1260	39		**39**	1133	33	
Detector 14	**40**	1369	46		**41**	1226	37		**42**	1120	33	
Detector 15	**43**	1561	53		**44**	1362	41		**45**	1234	35	
Detector 16	**46**	1620	52		**47**	1426	41		**48**	1286	34	
Detector 17	**49**	1581	51		**50**	1395	40		**51**	1260	35	
Detector 18	**52**	1374	47		**53**	1202	36		**54**	1086	31	

Table 15. Count rates of the 18 channels of the ArNM (07.02.2008).

	Number of Column	Average Count Rate (0.4us)	Std. Dev.	SUM	**Number of Column**	Average Count Rate (250us)	Std. Dev.	SUM	**Number of Column**	Average Count Rate (1250us)	Std. Dev.	SUM
Detector 1	**1**	2574	72	**43261**	**2**	2235	51	**38769**	**3**	1997	43	**35055**
Detector 2	**4**	2521	64		**5**	2249	52		**6**	2031	44	
Detector 3	**7**	2840	68		**8**	2528	54		**9**	2259	45	
Detector 4	**10**	2800	68		**11**	2495	54		**12**	2235	46	
Detector 5	**13**	2314	59		**14**	2092	48		**15**	1907	42	
Detector 6	**16**	2335	59		**17**	2074	47		**18**	1866	40	
Detector 7	**19**	2437	64		**20**	2169	51		**21**	1938	43	
Detector 8	**22**	2648	63		**23**	2368	50		**24**	2131	43	
Detector 9	**25**	2650	62		**26**	2392	50		**27**	2166	44	
Detector 10	**28**	2731	63		**29**	2469	51		**30**	2239	44	
Detector 11	**31**	2459	62		**32**	2209	52		**33**	2000	45	
Detector 12	**34**	2315	62		**35**	2055	49		**36**	1852	42	
Detector 13	**37**	2145	59		**38**	1910	46		**39**	1733	40	
Detector 14	**40**	1877	51		**41**	1723	44		**42**	1589	39	
Detector 15	**43**	2069	53		**44**	1900	45		**45**	1746	39	
Detector 16	**46**	2043	54		**47**	1861	45		**48**	1709	39	
Detector 17	**49**	2396	63		**50**	2146	50		**51**	1943	44	
Detector 18	**52**	2097	58		**53**	1886	48		**54**	1705	41	

4. The basic detecting unit of the SEVAN network

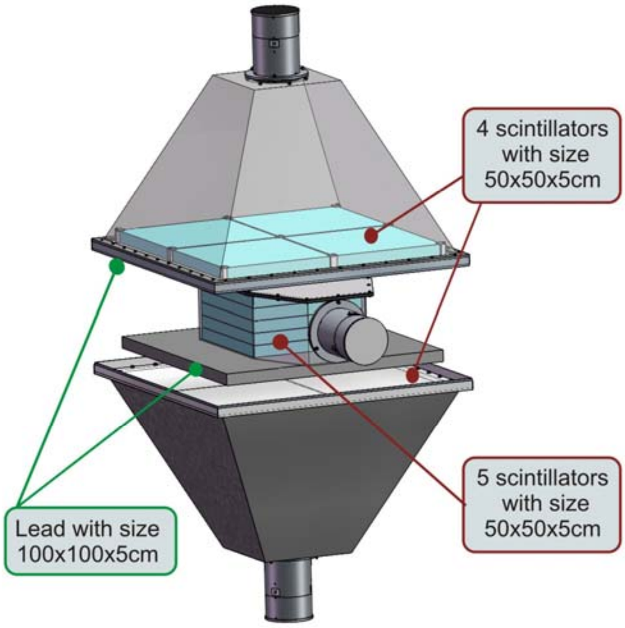

Figure 11 The basic detecting unit of the SEVAN network

The basic detecting unit of the SEVAN network (see Figure 11) is assembled from standard slabs of $50x50x5cm^3$ plastic scintillators. Between 2 identical assemblies of 100 x 100 x 5 cm^3 scintillators (four standard slabs) are located two 100 x 100 x 5 cm^3 lead absorbers and thick 50 x 50 x 25 cm^3 scintillator assembly (5 standard slabs). A scintillator light capture cone and Photo Multiplier Tube (PMT) are located on the top, bottom and the intermediate layers of detector. The detailed detector charts with all sizes are available from http://crdlx5.yerphi.am/.

At the Nor – Amberd research station of ASEC we are starting tests of the operation of the SEVAN detector prototype (SEVAN #1) with slightly reduced sizes: area of upper and lower 5-cm this scintillators are 0.65 m^2, instead of 1 m^2, and thickness of middle detector is 20 cm, instead of 25. Also we establish the SEVAN detector prototype (SEVAN #2) in the Yerevan. The dimensions of the upper and lower scintillaors are $1m^2$, and thickness of middle detector is 20 cm.

Incoming neutral particles undergo nuclear reactions in the thick 25 cm plastic scintillator and produce protons and other charged particles. In the upper 5 cm thick scintillator charged particles are registered very effectively; however for the nuclear interactions of neutral particles there is not enough substance. When a neutral particle traverses the top thin (5cm) scintillator, usually no signal is produced. The absence of the signal in the upper scintillators, coinciding with the signal in the middle scintillator, points to neutral particle detection. The coincidence of signals from the top and bottom scintillators indicates traversal of high energy muons. Lead absorbers improve efficiency of the neutral flux detection and filtered low energy charged particles. SEVAN world-wide network will consist of modules located in Croatia, Bulgaria, India (to be installe din 2008), Slovakia, Costa-Rica and Indonesia (to be installed in 2009). We present data from SEVAN module operated at Nor Amberd research station, another module is under construction in Yerevan at altitude 1000 m in CRD headquarters.

4.1. Structure of the information content from SEVAN detector

The following information is providing by SEVAN detector:

1. Count rates from the all 3 layers (see Table 16).
2. Count rates of the all coincidences of upper, middle and lower detectors (see Table 16 and Table 17).
3. Correlation matrix between all detected signals (Table 18)

The data is stored in http://crdlx5.yerphi.am/ASEC_Data/ADAS/sevan01/sevan1/

In the directory "DEFAULT" the following information is stored:

1. columns 1-3 - the count rates of all channels of the SEVAN. The count rates are posted in the Table 16;
2. column 4 unused (this channel we can use as input of the atmospheric pressure sensor).
3. columns 5-8 – the count rates of the coincidences of the all channels of the SEVAN. If we denote by the sign "1" signal from scintillator, and by sign "0" absence of signal, following combinations of the 3-layered detector output are stored: 110, 101, 011, 111 (see Table 16).

Table 16 Count Rates of the SEVAN channels and variances.

	Average	Standard deviation	Relative Error [%]
Upper Detector	9548	103	1.08
Middle Detector	4183	63	1.50
Lower Detector	5444	77	1.41
Coincidence 110	1052	32	3.04
Coincidence 101	512	23	4.44
Coincidence 011	676	25	3.69
Coincidence 111	1713	43	2.51

Table 17 Additional coincidences corresponding to different type particles by the SEVAN detector

	Average	Standard deviation	Relative Error [%]
Coincidence100 = Upper Detector – Coincidence110 – (low energy charged) Coincidence101 – Coincidence111	6271	82	1.31
Coincidence010 = Middle Detector – Coincidence110 – (neutral) Coincidence011 – Coincidence111	742	28	3.75
Coincidence001 = Lower Detector – Coincidence101 – (near horizontal) Coincidence011 – Coincidence111	2543	51	2.01

Table 18 Correlation between coincidences of the SEVAN 3 layers .

Coincidence	[110]	[101]	[011]	[111]	[100]	[010]	[001]
[110]	1						
[101]	0.034	1					
[011]	-0.018	-0.020	1				
[111]	-0.081	0.052	-0.055	1			
[100]	0.026	0.014	-0.087	0.067	1		
[010]	0.023	0.021	-0.026	0.019	0.057	1	
[001]	-0.022	0.102	-0.009	0.031	-0.072	-0.043	1

5. **MAKET-ANI Extensive Air Shower Detector.**

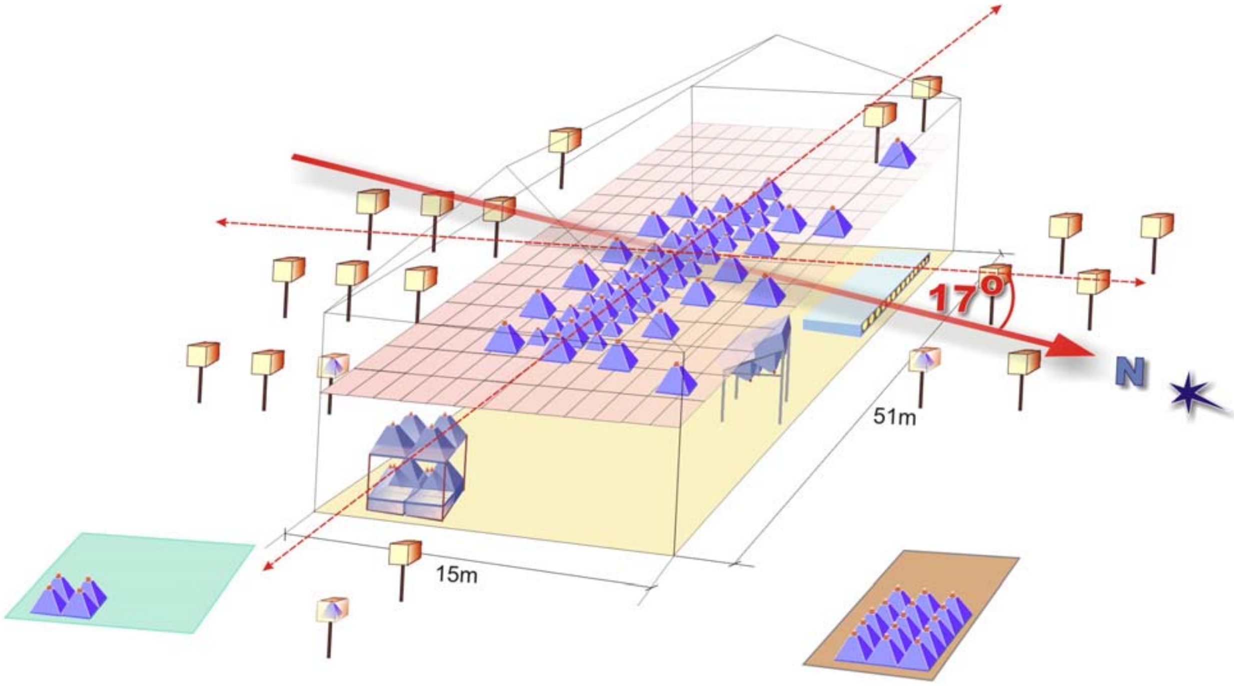

Figure 1 MAKET-ANI Extensive Air Shower Detector.

In the assembly of the ANI Cosmic Ray experiment (Danilova, et al., 1992), two detectors measuring the Extensive Air Showers (EAS) are operated on the Aragats research station. The main goal of the GAMMA (Garyaka, et al., 2002) and MAKET-ANI (Avakian, et al., 1986; Chilingarian, et al., 1999) detectors are to investigate the energy spectra of cosmic rays to understand the origin and accelerator mechanisms. Both detectors use the same particle density detection techniques to determine the number of electrons in the shower and infer the energy and type of the primary particle.

After obtaining and publishing final results of the MAKET-ANI (see Figure 1) experiment (Chilingarian, et al., 2007) the experiment was stopped for collecting high energy galactic cosmic rays. Some of the scintillators were used for rearranged smaller detector. Around the ASNT detector (consisted of four 60 cm thick scintillators and four 5 cm thick scintillators another 8 5 cm scintillators were arranged and attached to the 16 channel spectrum analyzer. We plan to test with this array new fast-timing technique to be used for new big array in Nor Amberd (Chilingarian, Hovsepyan, et al, 2007). Meanwhile new MAKET array provides following information:

1. 1 minute count rates of all 16 channels of the MAKET (see Table 19);
2. Count rate of the EAS triggering 8 and all 16 detectors;
3. Estimates of the variances of count rates of each MAKET channel, variances are calculated by 12 five-second count rates (see Table 21);
4. 16 x 16 correlation matrix of MAKET channels calculated by five-second count rates in 1 minute.

The data is stored in
http://crdlx5.yerphi.am/ASEC_Data/ADAS/maket/maket/
In the directory “DEFOULT” following information is stored:

1. Columns 1-16 - the count rates of all 16 MAKET channels: first 4 columns – from 60 cm scintillators, 5-16 columns – from 5 cm scintillator. The count rates are posted in the Table 19;

2. Columns 17-18 – the count rates corresponding to the EAS initiated triggers. 17th column corresponds to the coincidence of the first 8 channels (ASNT scintillators), 18th column corresponding to the coincidence in all 16 channels. The count rates are posted in the Table 20;
3. Columns 19-34 – the variances of 16 channels, see Table 21;
4. Columns 35-154 – the correlation matrix.

In the directories "spectrum" following information is stored:
1. spectrum1, … spectrum4 the histograms of the energy releases in thick 60 cm scintillator are stored. In files with extension;
2. spectrum5, … spectrum16 the histograms of energy releases in 5 cm thin scintillators are stored;

In the CRD local server available files with following information:
- In the files with "events" extension is related to the Extensive Air Showers (EAS). The logical software trigger selects events when signals are more than in 8 detectors.

Table 19 Count Rates of the MAKET channels, variances and relative errors.

Detector	Average	Standard deviation	Relative error [%]
Detector 1 (60cm)	37973	201	0.53
Detector 2 (60cm)	29869	185	0.62
Detector 3 (60cm)	33244	188	0.57
Detector 4 (60cm)	32074	164	0.51
Detector 5	23732	152	0.64
Detector 6	28100	167	0.59
Detector 7	17125	146	0.85
Detector 8	24845	174	0.70
Detector 9	22956	144	0.63
Detector 10	18313	140	0.76
Detector 11	23722	159	0.67
Detector 12	18901	148	0.78
Detector 13	22589	152	0.67
Detector 14	19492	134	0.69
Detector 15	22964	152	0.66
Detector 16	21154	144	0.68

Table 20 Count Rates of the MAKET EAS initiated triggers, variances and relative errors.

Detector	Average	Standard deviation	Relative error [%
Coincidence in thirst 8 channels	20	4	21.02
Coincidence in all 16 channels	5	2	41.95

Table 21 Mean value of the variance, its variance and relative error calculated by 5-sec count rates of 1 minute time span (total 12 5-dec count rates).

Detector	Average	Standard deviation	Relative error [%]
Detector 1 (60cm)	53	11	21.46
Detector 2 (60cm)	49	10	21.06
Detector 3 (60cm)	52	12	22.63
Detector 4 (60cm)	50	11	21.37
Detector 5	44	10	21.87
Detector 6	47	10	22.18
Detector 7	37	8	20.79
Detector 8	45	11	23.28
Detector 9	43	9	20.85
Detector 10	38	8	21.16
Detector 11	43	9	20.96
Detector 12	39	8	20.66
Detector 13	42	9	20.62
Detector 14	39	8	21.22
Detector 15	43	9	21.68
Detector 16	41	8	20.50

6. Aragats Multidirectional Muon Monitor (AMMM)

The Aragats Multidirectional Muon Monitor (AMMM) consists from 2 layers of the scintillation detectors. 29 scintillation detectors (each detector have 1m^2 surface and 5cm thickness), located on top of the top of ANI concrete calorimeter and 100 the same type detectors 14 m below (under 4m concrete and 7m soil), as shown in Figure 13 and 14. Zenith angle between axes of AMMM and direction to South pole is ~-17º. Count rate in the upper detectors is ~28000 counts per minute and variance ~170. Count rate of each of 1 m^2 scintillators in the underground hall(high energy muons with energy threshold 5 GeV) is ~3000 counts per minute and variance ~55. The relative accuracy of 1-minute count rates of underground high energy muon detector is ~0.2%, of the low energy muons and electrons on surface ~ 0.12%.

The new electronics will be installed in the summer 2008. The present DAQ consists of scalers attached to on-line PC by COM port.

AMMM data is available from SKYNET local server. Data from first 59 channels of the NAMMM lower layer you can find by this link \\soul\ASEC_data\amet. The last 30 channels of the NAMMM lower layer you can find here \\soul\ASEC_data\arme in the files with extension .ame. The first 30 columns are corresponding to the lower layer AMMM, the second 29 columns corresponding to the upper layer AMMM.

In Figure 15 we present the daily variations of the high energy secondary muons averaged over 21 days.

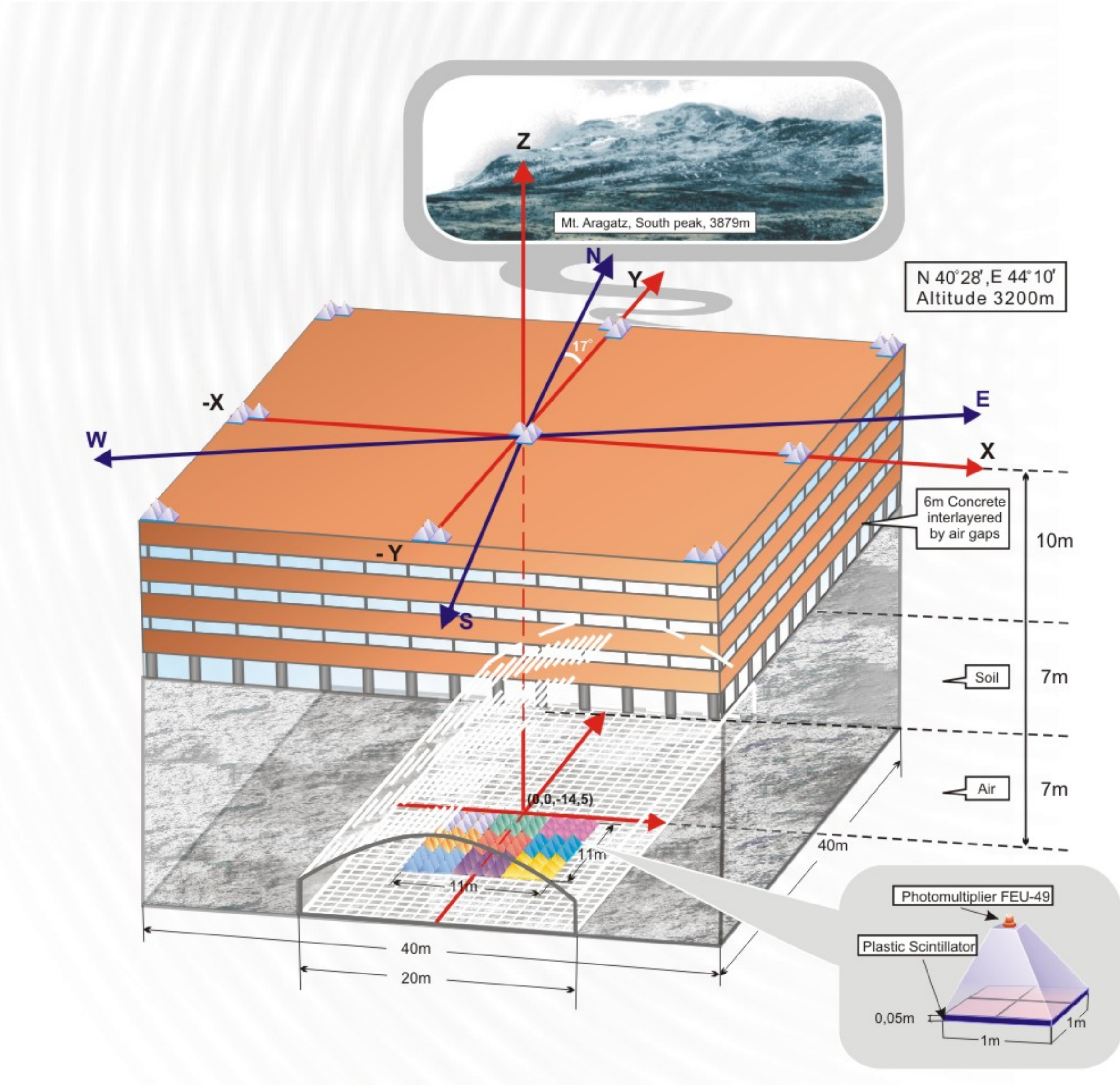

Figure 1: Aragats Multidirectional Muon Monitor (AMMM).

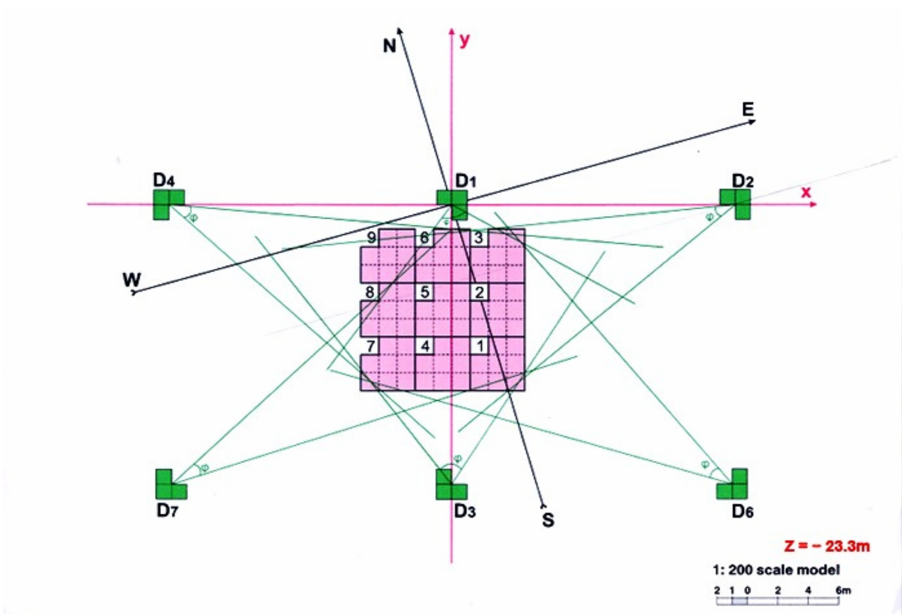

Figure 2 Projection of the AMMM on the X-Y plane

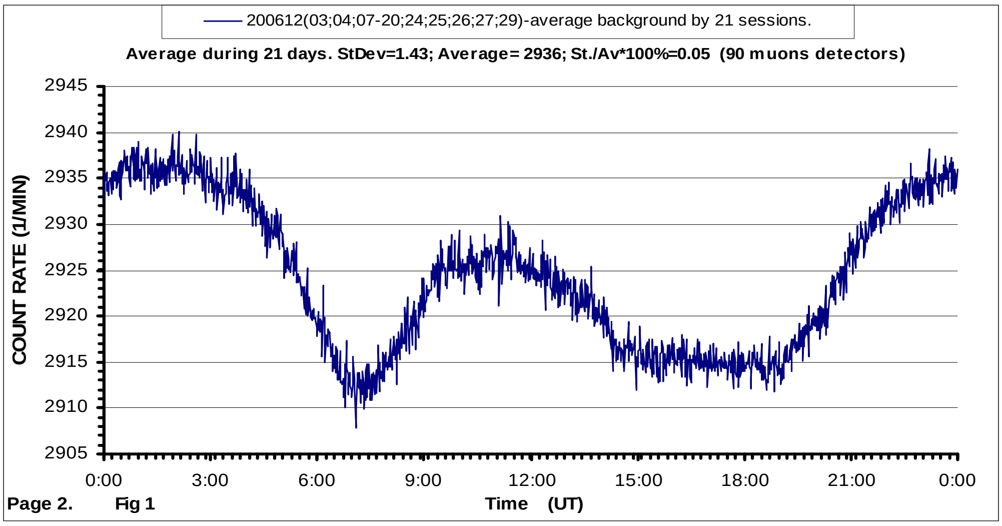

Figure 3 The "daily wave" – the time variations of the count rate of high energy muons.

In tables 22 and 23 we present averaged count rates as measured at 8 December 2007 and total number of muons measured by each detector per day. Total 248,292,843 muons were detected.

Table 22 Average minute count rates and standard deviations of 5 GeV muons measured at 8 December 2007

Nº	Average	Standard deviation	Relative error [%]	Nº	Average	Standard deviation	Relative error [%]	Nº	Average	Standard deviation	Relative error [%]
1	2914	43.1	1.48%	**31**	2939	52.2	1.78%	**61**	3003	54.4	1.88%
2	3052	55.9	1.83%	**32**	2875	55.7	1.94%	**62**	2883	55.6	1.93%
3	3027	56.7	1.87%	**33**	2834	56.3	1.99%	**63**	2687	54.9	2.04%
4	2804	53.5	1.91%	**34**	2749	55.0	2.00%	**64**	2854	59.5	2.08%
5	2997	56.9	1.90%	**35**	2933	55.8	1.90%	**65**	2931	56.2	1.92%
6	3013	55.0	1.83%	**36**	2704	53.6	1.98%	**66**	2674	52.4	1.96%
7	2957	54.5	1.84%	**37**	2854	55.6	1.95%	**67**	3049	63.5	2.08%
8	2829	55.5	1.96%	**38**	2834	54.8	1.93%	**68**	2832	59.9	2.12%
9	2896	53.6	1.85%	**39**	2873	52.6	1.83%	**69**	2988	52.8	1.77%
10	2930	54.7	1.87%	**40**	2768	55.1	1.99%	**70**	2837	53.9	1.90%
11	2945	55.3	1.88%	**41**	2756	53.0	1.92%	**71**	2732	55.1	2.02%
12	2912	54.0	1.86%	**42**	2683	53.6	2.00%	**72**	2708	50.8	1.88%
13	2800	53.6	1.91%	**43**	2845	58.3	2.05%	**73**	2827	51.0	1.80%
14	2785	54.1	1.94%	**44**	2773	53.4	1.93%	**74**	2844	56.1	1.97%
15	2972	55.5	1.87%	**45**	2713	55.5	2.05%	**75**	2608	52.8	2.03%
16	2815	53.5	1.90%	**46**	2771	55.2	1.99%	**76**	3042	56.7	1.86%
17	2874	55.0	1.91%	**47**	3006	56.4	1.88%	**77**	3112	58.5	1.88%
18	2904	54.5	1.88%	**48**	3105	56.4	1.82%	**78**	3061	55.8	1.82%
19	2917	56.2	1.93%	**49**	3047	56.4	1.85%	**79**	2824	56.9	2.01%
20	2753	54.1	1.97%	**50**	3087	58.5	1.90%	**80**	2988	52.8	1.77%
21	2858	54.2	1.90%	**51**	2942	49.6	1.69%	**81**	2950	56.8	1.93%
22	2824	53.7	1.90%	**52**	3053	56.9	1.86%	**82**	3014	56.6	1.88%
23	2704	53.6	1.98%	**53**	2950	56.5	1.92%	**83**	3214	57.2	1.78%
24	2833	54.3	1.92%	**54**	3148	58.8	1.87%	**84**	3069	59.4	1.94%
25	2765	53.8	1.94%	**55**	2813	54.7	1.94%	**85**	3063	57.7	1.88%
26	2810	55.7	1.98%	**56**	2871	55.4	1.93%	**86**	3133	58.5	1.87%
27	2686	50.7	1.89%	**57**	2964	55.8	1.88%	**87**	2934	58.1	1.98%
28	2706	53.2	1.96%	**58**	3070	55.3	1.80%	**88**	3048	54.7	1.79%
29	2799	54.6	1.95%	**59**	2785	55.0	1.98%	**89**	2847	52.3	1.84%
30	2883	54.7	1.90%	**60**	2717	54.4	2.00%				

Table 23 One day count rates and standard deviations of 5 GeV muons measured at 8 December 2007

№	$\sum_{n=1}^{1440}$	$\sigma_i = 1/\sqrt{\sum}$	№	$\sum_{n=1}^{1440}$	$\sigma_i = 1/\sqrt{\sum}$	№	$\sum_{n=1}^{1440}$	$\sigma_i = 1/\sqrt{\sum}$
1	4196468	0.0488%	**31**	4232101	0.0486%	**61**	4324100	0.0481%
2	4395304	0.0477%	**32**	4139766	0.0491%	**62**	4150894	0.0491%
3	4359005	0.0479%	**33**	4080938	0.0495%	**63**	3869546	0.0508%
4	4037325	0.0498%	**34**	3958483	0.0503%	**64**	4109263	0.0493%
5	4315526	0.0481%	**35**	4222960	0.0487%	**65**	4219990	0.0487%
6	4338958	0.0480%	**36**	3893592	0.0507%	**66**	3851007	0.0510%
7	4258254	0.0485%	**37**	4110259	0.0493%	**67**	4390325	0.0477%
8	4073309	0.0495%	**38**	4081318	0.0495%	**68**	4077850	0.0495%
9	4169796	0.0490%	**39**	4137306	0.0492%	**69**	4303104	0.0482%
10	4218662	0.0487%	**40**	3986352	0.0501%	**70**	4085042	0.0495%
11	4240291	0.0486%	**41**	3968941	0.0502%	**71**	3933727	0.0504%
12	4192812	0.0488%	**42**	3863947	0.0509%	**72**	3900099	0.0506%
13	4032229	0.0498%	**43**	4096364	0.0494%	**73**	4071561	0.0496%
14	4010753	0.0499%	**44**	3992580	0.0500%	**74**	4095402	0.0494%
15	4279079	0.0483%	**45**	3907415	0.0506%	**75**	3754887	0.0516%
16	4053002	0.0497%	**46**	3989798	0.0501%	**76**	4381165	0.0478%
17	4138683	0.0492%	**47**	4328704	0.0481%	**77**	4481856	0.0472%
18	4181801	0.0489%	**48**	4471243	0.0473%	**78**	4408270	0.0476%
19	4199887	0.0488%	**49**	4387797	0.0477%	**79**	4066982	0.0496%
20	3963823	0.0502%	**50**	4445565	0.0474%	**80**	4303104	0.0482%
21	4115385	0.0493%	**51**	4236352	0.0486%	**81**	4248538	0.0485%
22	4067173	0.0496%	**52**	4396528	0.0477%	**82**	4340346	0.0480%
23	3894107	0.0507%	**53**	4247376	0.0485%	**83**	4628072	0.0465%
24	4079820	0.0495%	**54**	4533420	0.0470%	**84**	4420002	0.0476%
25	3980961	0.0501%	**55**	4050083	0.0497%	**85**	4411247	0.0476%
26	4046710	0.0497%	**56**	4134758	0.0492%	**86**	4511576	0.0471%
27	3868109	0.0508%	**57**	4268051	0.0484%	**87**	4225168	0.0486%
28	3897071	0.0507%	**58**	4420483	0.0476%	**88**	4389114	0.0477%
29	4031055	0.0498%	**59**	4010297	0.0499%	**89**	4099514	0.0494%
30	4152082	0.0491%	**60**	3912626	0.0506%			

In Table 24 we present analogical characteristics for 29 plastic scintillators located on the top of ANI calorimeter.

Along with 1-minute data from ASEC monitors available from MSQL data base, the summary of daily plots can be observed from http://crdlx5.yerphi.am/ADVANCED_DAILY_IMAGES/. Same plots are also available from mirror site http://aragats.am

CRD continuously enlarge operating particle detectors number. In 2008 we plan to install several SEVAN modules in Yerevan and Burakan village. A new type multilayered detector is under testing in Yerevan headquarters. 10 one cm thick plastic scintillators interlayer by 1 cm thick lead will measure muon and hadron energy by detecting electromagnetic and hadron showers. New electronics and new type of micro computers will be used to make Data Acquisition from particle detectors faster and multi-functional.

New user-friendly interface to ASEC monitor data, named DVIN-4, is under final tuning and will highly improve physical analysis possibilities.

Table 24 Averaged 1 minute and dayly count rates of surface low energy charged flux measured at 8 December 2007

№	Average	Standard deviation	Relative error [%]
1	29279	180	0.62%
2	28238	249	0.88%
3	28721	261	0.91%
4	29703	223	0.75%
5	29283	181	0.62%
6	28333	256	0.90%
7	29948	247	0.82%
8	28859	301	1.04%
9	29119	244	0.84%
10	29076	178	0.61%
11	28789	282	0.98%
12	28460	166	0.58%
13	29077	178	0.61%
14	29895	229	0.77%
15	28972	250	0.86%
16	28734	245	0.85%
17	29056	240	0.83%
18	27832	248	0.89%
19	29461	230	0.78%
20	29767	236	0.79%
21	28782	229	0.80%
22	27445	247	0.90%
23	29092	238	0.82%
24	29076	177	0.61%
25	28207	281	0.99%
26	29053	224	0.77%
27	28370	257	0.91%
28	28111	175	0.62%
29	28491	248	0.87%

№	$\sum_{n=1}^{1440}$	$\sigma_i = 1/\sqrt{\sum}$
1	42161758	0.0154%
2	40662397	0.0157%
3	41357704	0.0155%
4	42772070	0.0153%
5	42167188	0.0154%
6	40799310	0.0157%
7	43124876	0.0152%
8	41557256	0.0155%
9	41931409	0.0154%
10	41870013	0.0155%
11	41455964	0.0155%
12	40982046	0.0156%
13	41871011	0.0155%
14	43049245	0.0152%
15	41719295	0.0155%
16	41377597	0.0155%
17	41840189	0.0155%
18	40078730	0.0158%
19	42423917	0.0154%
20	42864930	0.0153%
21	41446634	0.0155%
22	39520922	0.0159%
23	41891844	0.0155%
24	41868918	0.0155%
25	40618066	0.0157%
26	41835649	0.0155%
27	40853231	0.0156%
28	40480268	0.0157%
29	41026404	0.0156%

7. References

- Avakian V.V., Bazarov E.B., et. al., (1986), VANT, ser. Tech. Phys. Exp., 5(31), p.1.
- Beglaryan A.S., Bujukyan S.P., et al., (1989) Scientific Publication of YerPhI, 1197 (74).
- Chilingarian A., Hovsepyan G., Gharagyozyan G., et al.: (1999) The EAS Size Spectrum measured at ANI Cosmic Ray Observatory in the region of Knee, 26th International Cosmic Ray Conference, Salt Lake City, vol 1, p. 240-243.
- Chilingarian, A., Avakyan, K., Babayan, V., et al.: (2003) Aragats Space-Environmental Center: status and SEP forecasting possibilities, J. Phys. G: Nucl. Part. Phys., Vol. 29, p. 939-952.
- Chilingarian A., Gharagyozyan G., Hovsepyan G., et al.: (2004) Light and heavy cosmic-ray mass group energy spectra as measured by the MAKET-ANI detector, Astrophysical Journal, 603, p. L29–L32.
- Chilingarian A., Arakelyan K., Avakyan K., et al.: (2005) Correlated measurements of secondary cosmic ray fluxes by the Aragats Space – Environmental Center monitors, Nucl. Instr. and Meth. A 543, p. 483-496.
- Eghikyan A., Chilingarian A., (2005) Data Visualization Interactive Network for the Aragats Space – Environmental Center, 2rd International Symposium SEE-2005, Nor-Amberd, Armenia, p. 245-251. (http://crdlx5.yerphi.am/DVIN/)
- Chilingarian A., Hovsepyan G., et al, (2007)Study of Extensive Air Showers and Primary Energy Spectra by MAKET-ANI Detector on Mountain Aragats, Astroparticle Physics **28**, 58-71
- Chilingarian A., Hovsepyan G., et al, Research on Galactic Cosmic Rays from the “knee” to the “cutoff” (10^{16} -10^{19}) eV at the Aragats Cosmic Ray Observatory; *Measurements of the ultra -high energy Cosmic Rays by hybrid particle detectors located on the Earth surface, report on JENAM-2007 conference.*
- A.Chilingarian et al, (2007) Study of Extensive Air Showers and Primary Energy Spectra by MAKET-ANI Detector on Mountain Aragats, Astroparticle Physics 28, p. 58-71.
- Dorman L.I., (1975) Variations of the Galactic Cosmic Rays, Publishing house of the Moscow State University.
- Danilova T.V., Danilova E. A., Erlikin A. B., et al.: (1992) The ANI experiment: on the investigation of interactions from hadrons and nuclei in the energy range 103–105 TeV, Nucl. Instr. and Meth. A 323, p. 104-107.
- Garyaka A.P., Martirosov R.M., Procureur J., et al.: (2002) The cosmic ray energy spectrum around the knee measured with the GAMMA array at Mt. Aragats, J. Phys. G: Nucl. Part. Phys. 28, p. 2317-2328.
- Moraal H., Belov A., Clem J.M.: (2000) Design and co-Ordination of Multi-Station International Neutron Monitor Networks, Space Science Reviews 93, p. 285-303.
- Tsuchiya et al. (2001), NIM, **A 463**, 183 – 193.